[redacted]

Cosmic Ray Physics Report

LUIP-CR-74-14

October 1974

PION AND PROTON EMISSION IN INTERACTIONS INDUCED BY RELATIVISTIC HEAVY NUCLEI WITH $Z \geq 12$

B. Jakobsson, R. Kullberg and I. Otterlund

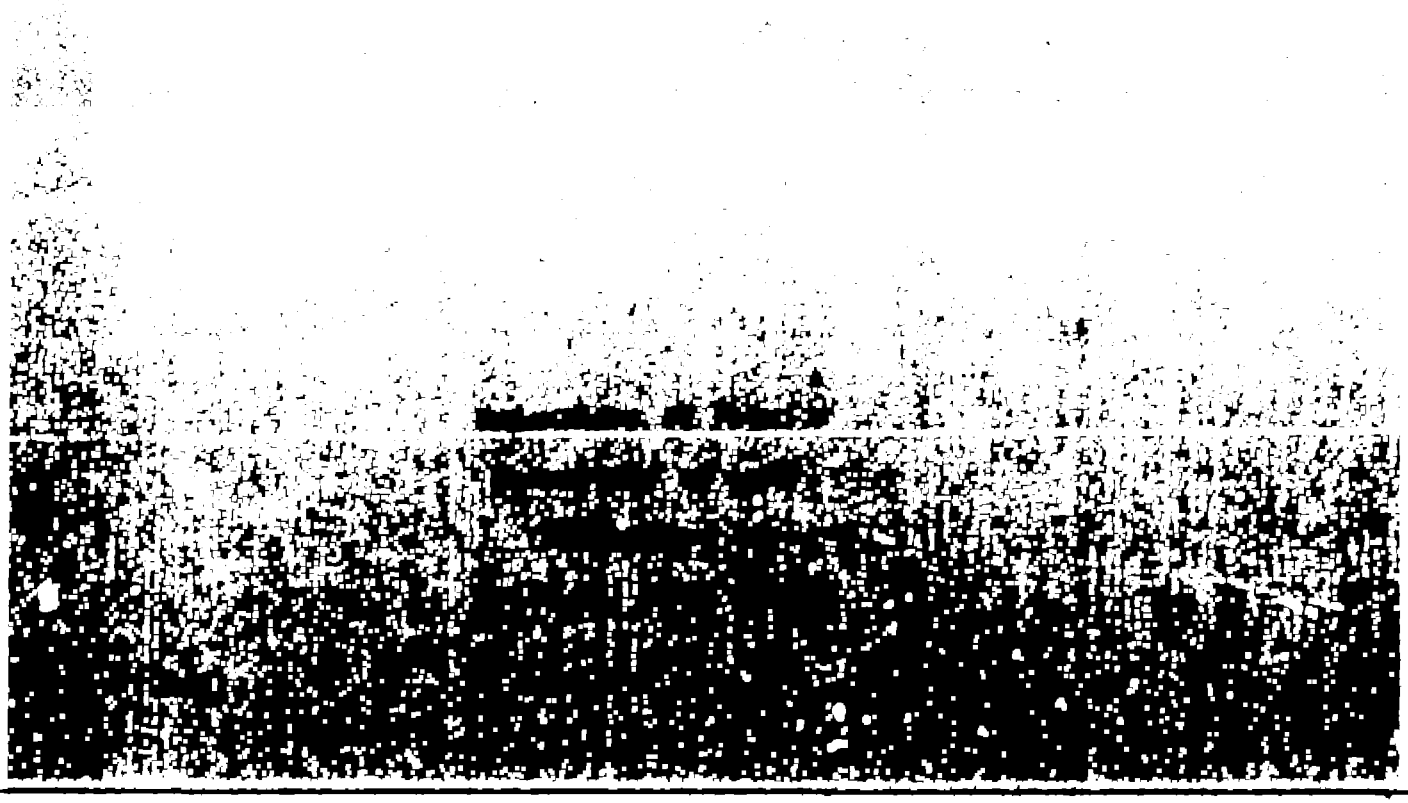

PION AND PROTON EMISSION IN INTERACTIONS INDUCED BY RELATIVISTIC HEAVY NUCLEI WITH $Z \geq 12$

B. Jakobsson, R. Kullberg and I. Otterlund

Contents

Pion and Proton Emission in Interactions Induced by Relativistic Heavy Nuclei with $Z \geq 12$

B. Jakobsson, R. Kullberg and I. Otterlund
Department of Physics, University of Lund, Lund, Sweden.

Abstract

The emission of pions and protons in interactions between heavy nuclei from the cosmic radiation ($12 \leq Z \leq 26$) and photoemulsion nuclei has been studied. The angular and energy distributions of target protons are similar to corresponding distributions in proton-nucleus interactions for emission angles $\geq 30^{\circ}$. In heavy ion interactions a forward peak of high energy target protons ($E \geq 200$ MeV) is observed. The energy spectrum of target protons for angles $< 30^{\circ}$ is remarkably flat for heavy ion interactions.

For increasing disintegration of the target nucleus the number of produced pions per emitted recoil target proton is almost constant in heavy ion interactions, while it decreases rapidly in proton-nucleus interactions. The $\log \mathrm{tg}\,\theta$ distributions of pions have small standard deviations even in interactions with a large target disintegration.

1. Introduction

Nucleon-nucleus (n-N) interactions at high energy have been described with models assuming a first stage of free nucleon-nucleon (n-n) and pion-nucleon (π-n) collisions fol-

lowed by the emission of particles from an excited residual nucleus in equilibrium. This simple model has been modified by introducing preequilibrium emission (1,2). In a first approximation, heavy ion interactions (N-N) have been treated as a superposition of independent n-N collisions (3). Recent papers have however pointed to large differences from this simple view, especially for interactions with a complete target nucleus breakup (4). Non-statistical models, for instance the breakup model (5) and the hydrodynamical model (6) seem to give a more adequate description of these collisions. Feshbach and Huang (7) have suggested a model where the target nucleus only acts as an injector of energy for the incident nucleus.

In this report we have studied the emission of protons and charged pions in relativistic interactions between heavy incident nuclei from the cosmic radiation and emulsion nuclei. The emission of multiply-charged particles has been studied in an earlier investigation (8).

2. Experimental Details

In this investigation two Ilford G5 emulsion stacks were used. The criteria for selection of interactions with primaries having a charge of $12 \leq Z \leq 26$ ($\langle Z \rangle \approx 19$) and a kinetic energy > 1 GeV/nucleon are given in Ref. 8. Separation between different types of secondary particles was performed by measuring range, restricted energy loss (REL) and the rate of change of REL whereever possible. REL was determined by gap counting or by mean blob length measurements including a correction for the dip angle, which takes into consideration the exponential distribution of the gaplengths and the overlap of grains.

The commonly used classification of tracks in emulsion is:

1. Black tracks, N_b, $I \geq 6.8\ I_o$
2. Grey tracks, N_g, $1.4 \leq I < 6.8\ I_o$
3. Shower tracks, N_s, $I < 1.4\ I_o$,

where I_o is the minimum energy loss for a singly charged particle.

Heavy prong-producing particles (N_h) are low energy mesons, hydrogen, helium and heavier nuclei. We identified hydrogen nuclei with $9 \leq E_p < 400$ MeV for dip angles $\rho \leq 60^o$. In this sample there is a small perturbation of pions with REL corresponding to proton energies 235 - 400 MeV. The dip angle corrections of the energy- and angular distributions were determined from the distributions for emission angles 60-120° ($\rho \leq 60^o$) and the total number of particles with $\rho > 60^o$.

Pions with $E_{\pi^\pm} \leq 35$ MeV and helium nuclei with $E_{He} \geq 36$ MeV could be identified. Isotopic separation of hydrogen nuclei was in general not possible, and subsequently we have treated all hydrogen nuclei as protons (9,10).

The identification of the target nuclei is described in Ref. 8.

3. Emission of Protons in the Energy Interval 9-400 MeV

3.1 Angular Distributions

Protons with energies < 400 MeV are almost exclusively associated with the target nuclei. To obtain distributions of these protons we have corrected for the disturbance of pions. Since we could not separate pions with $E_{\pi^\pm} > 35$ MeV from protons, we have estimated a pion energy distribution from the models of pion production discussed in chapter 4. The number of pions with $E_{\pi^\pm} < 35$ MeV predicted from this estimation agree within the limits of error with the experimental number. According to this estimation $N_{\pi^\pm}(35\text{-}60\ \text{MeV}) = 1.2\ N_{\pi^\pm}(4\text{-}35\ \text{MeV})$.

The angular distribution of protons in three different

energy intervals is shown in Fig. 1. The small admixture of protons from light target events does not affect the total distributions. Predictions from evaporation theory using reasonable values of the nuclear temperature, the reduced Coulomb barrier and the recoil velocity are in agreement with the angular distribution of protons between 9 and 30 MeV (T = 7 MeV, V = 1 MeV, $\beta_{//}$ = 0.015 and $\beta_{\perp}$ = 0.007). Similar agreement has been reported in several articles describing interactions induced by hadrons or photons.

In the energy interval $30 \leq E_p < 400$ MeV a pronounced peak of protons is developed in the forward direction. The peak increases with increasing proton energy. Fig. 2 shows that a similar peak is not obtained in p-N interactions.

Angular distributions obtained in hadron-nucleus interactions can be described by the formula

$$N = N_o \exp(b \cos \Theta) \qquad [1]$$

This simple distribution can only describe the proton distribution in N-N interactions for $\cos \Theta \leq 0.8$. The large excess of particles with $\cos \Theta > 0.8$ is mainly due to protons with $E_p > 235$ MeV (Fig. 1).

Table 1

Type of interaction	E_{inc}	b	Reference
N-N	> 1.0 GeV/n	1.3 ± 0.1	This work, $\cos\Theta \leq 0.8$
p-N	6.2 GeV	0.94 ± 0.05	11
	22.5 GeV	0.79 ± 0.12	11
	2.26 GeV 19.5 GeV }	≈ 0.96	12
π-N	60 GeV	$0.96^{+0.09}_{-0.06}$	12

Table 1 gives values of the constant b obtained from angular distributions of grey tracks for interactions with Ag-Br targets. In p-N and N-N interactions b is independent of the incident energy. Thus the excess of protons with small angles in the N-N interactions studied cannot be caused by the fact that the beam of incident particles is not monoenergetic.

3.2 Energy Distributions

In Fig. 3 we compare the proton energy spectrum with that obtained in p-N interactions at 950 MeV (13). Since the energy spectrum of grey track-producing protons is almost independent of the incident energy in the GeV region (13,14,15) it is reasonable to compare with this p-N spectrum. For energies $\geq$ 100 MeV the energy spectrum decreases more rapidly in p-N than in N-N interactions. The p-N distribution has about a 7 % disturbance of pions (13). A correction for this pion disturbance would make the difference even more pronounced.

The energy distribution of protons for two different angular intervals a) $\theta < 30^{\circ}$ and b) $70 \leq \theta < 110^{\circ}$ are demonstrated in Fig. 4. The distributions are compared with the corresponding spectra for p-N collisions at 2.7 GeV (16). Since the median energy in the N-N sample is 2.4 GeV/nucleon, the comparison with p-N collisions at 2.7 GeV is relevant. Interactions with Ag or Br targets have been selected in both investigations. A second comparison has been made with intranuclear cascade calculations by Bertini (17) for p-N collisions. The agreement between the calculations and experimental p-N distributions is excellent. The N-N spectrum for $\theta < 30^{\circ}$, which is almost flat, differs significantly from the p-N spectrum. For $70 \leq \theta < 110^{\circ}$ the N-N spectrum as well as the p-N spectrum decrease rapidly for proton energies $\leq$ 200 MeV.

4. Angular Distributions of Pions and Fast Protons

Angular distributions of shower particles in p-N interactions with a small number of heavy prongs are similar to corresponding p-p distributions. However, for increasing N_h-values the deviation from p-p distributions becomes more and more obvious. In this chapter we compare angular distributions of pions and fast ($\beta > 0.7$) protons emitted in N-N interactions with corresponding p-p distributions.

4.1. Emission of Pions and Protons in p-p Interactions

Experimental cm angular distributions obtained in p-p interactions (18,19,20) have been transformed into laboratory angular distributions. The following transformation including the Lorenz invariant transverse momentum ($P_\perp$) has been used:

$$\operatorname{tg} \Theta_{lab} = \frac{\sin \Theta_{cm}}{\gamma_c \cos \Theta_{cm} + (\beta_c^2 \gamma_c^2 E_o^2 \sin^2 \Theta_{cm} / P_\perp^2 + \beta_c^2 \gamma_c^2)^{1/2}} \quad [2]$$

where E_o is the rest energy of the particle,

β_c is the velocity of the cm system in the laboratory frame and

β_{cm} is the velocity of the particle in the cm system.

The cm angular distributions of charged pions from the different reaction channels obtained by Almeida et al. (18) as well as an isotropic cm emission have been used. In the literature various analytic expressions are given for the $P_\perp$ distribution of pions emitted in p-p interactions. We have tested three $P_\perp$ distributions combined with the experimental anisotropic cm angular spectrum at 10 GeV. Logtg Θ distributions from these calculations as well as a calculation using a Maxwellian distribution for the total momentum are shown in Fig. 5. The logtg Θ distributions based upon the anisotropic angular spectrum are almost identical. The standard deviation (σ) is 0.51. If

we instead assume an isotropic cm production of pions, the standard deviation is reduced to 0.42. Subsequently, the $p_\perp$ distribution

$$N \sim p_\perp \exp(-Bp_\perp^2) \quad \langle p_\perp \rangle = 0.35 \text{ GeV/c} \qquad [3]$$

is used. A similar study of the protons emitted in inelastic p-p interactions shows that

$$N \sim p_\perp^2 \exp(-Bp_\perp) \quad \langle p_\perp \rangle = 0.5 \text{ GeV/c} \qquad [4]$$

as well as a Maxwellian $p_\perp$ distribution give almost identical logtg Θ distributions. Subsequently, the former distribution for protons is used.

In Fig. 6 calculated logtg Θ distributions of protons and pions from p-p interactions at 2 and 10 GeV are shown. Curve 2 shows the proton distribution from elastic p-p scattering. At 2 GeV we have used experimental $\frac{d\sigma}{d\Omega}$ distributions given in Refs. 20 and 21 and at 10 GeV the expression

$$\frac{d\sigma}{dt} = \text{const} \exp(-10.0\beta_{cm}^2 p_\perp^2) \qquad [5]$$

where t is the four-momentum transfer (22). The logtg Θ distributions of protons and pions emitted in inelastic p-p reactions are represented by curves 3 and 4. In these calculations we have used cm angular distributions from the different reaction channels obtained by Fickinger et al. (20) and Almeida et al. (18).

Fig. 6 also shows the angular distribution of protons emitted from excited projectile fragments in N-N interactions (curve 1). For energies > 1 GeV the pion angular distribution of nucleon-nucleon interactions can be approximated with the p-p distribution. However, in heavy ion interactions Fermi motion and secondary nucleon and meson induced reactions are important. These effects tend to increase σ. Furthermore collective reactions are likely to occur, and also shock wave reaction

mechanisms may be of importance (23).

4.2. Comparisons between the Emission of Pions and Fast Protons in p-p and N-N Interactions

In Fig. 7 logtg θ distributions of shower particles in N-N interactions are presented. Interactions with $N_h > 1$ are divided into five subgroups according to the charged pion multiplicity. The curves show angular distributions of pions in p-p interactions (18,19,20) normalized to the experimental number of charged pions ($N_{\pi^\pm}$). The energy of the incident proton is chosen in order to give agreement between the curve and the part of the distribution with large angles. The number of projectile protons (N_p) has been estimated from the expression

$$N_p = Z_{inc} - \Sigma Z_{fr} \qquad [6]$$

where Z_{fr} is the charge of projectile fragments with $Z \geq 2$. N_h and N_p is a measurement of the disintegra ion of the interacting nuclei. For an increasing impact parameter an increasing relative number of protons with small momentum transfer is expected. This is demonstrated in Figs. 7a-e. The number of particles with small angles increases with decreasing values of $\langle N_h \rangle$ and $\langle N_p \rangle$. In interactions with $N_h \leq 1$ (mainly hydrogen targets) (8) a dominant part of the fast protons has been evaporated from excited projectile fragments. This is shown in Fig. 7f where an evaporation distribution weighted over the cosmic ray spectrum is presented.

The logtg θ distribution in Fig. 7a has a remarkably small standard deviation ($\sigma = 0.46$) in spite of the fact that both interacting nuclei are almost totally disintegrated. Even if all interactions with $N_h \geq 28$ are considered σ does not increase to more than 0.50. This suggests that most pions are produced in the first encounters between the interacting hadrons. A special

study of the three largest stars has been made (Fig. 8). The angular distribution of pions produced in p-p interactions at 10 GeV normalized to the number of pions in the N-N interactions is also shown. In spite of the fact that the N-N distributions contain a rather large fraction of protons, σ is less than or equal to the σ-value of the pion distribution in p-p interactions. The discrepancy between the curve and the experimental histograms from the individual interactions seems to be restricted to a small logtg Θ interval and indicates a large transverse momentum transfer to projectile protons. In spite of the large value of $\langle N_h \rangle$ the $\langle \text{logtg } \Theta \rangle$ value is the same as the value in free p-p interactions. This result is not found in p-N interactions (24), where $\langle \text{logtg}\Theta \rangle_{p-N} - \langle \text{logtg}\Theta \rangle_{p-p}$ increases with increasing N_h.

The mean number of charged pions per incident nucleon in these collisions is ≈ 3. The extreme assumption that all incident nucleons individually interact with one target nucleon implies from $\langle n_{ch} \rangle_{p-p}$ an incident energy of at least 30 GeV/nucleon (25). The positions of the maxima of the logtg Θ distributions and the cosmic ray energy spectrum indicate however a much lower energy. Thus interactions with large pion multiplicity can not be approximated with superposition of independent n-n or n-N collisions.

4.3. Angular Distributions of Pions and Fast Protons in p-p p-N and N-N Interactions

Fig. 9 shows the cos Θ distribution of pions and fast protons in the whole sample. A calculated distribution of pions emitted in p-p interactions, assuming an isotropic cm emission, normalized to the number of pions, is also shown. In the calculations we took into account the cosmic ray energy spectrum

and the energy dependence of the charged pion multiplicity. A distribution of shower particles emitted in p-N interactions at 9 GeV (11) is also shown. The number of pions in this distribution has been estimated assuming a mixture of 0.7 protons per interaction. A normalization giving the same number of pions in the two distributions has been used. The p-N distribution does not include all interactions with $N_h \geq 8$, but this lack of events can only slightly affect the angular distribution of shower particles.

For $\cos\theta < 0.8$ there is good agreement between the experimental distributions and the distribution estimated from an isotropic cm emission. The proton contribution, which is concentrated to angl $s < 25^\circ$ in the N-N sample ($\cos\theta > 0.9$), is studied separately in the figure. The proton contribution can be observed at least to angles as large as 50°.

5. Characteristics of the Disintegration of the Interacting Nuclei

In order to investigate the dependence of the particle emission on the breakup of the interacting nuclei, we have divided the collisions into different classes. Multiplicities of secondary particles in N-N interactions with different degree of target breakup have been studied and compared to multiplicities in p-N collisions.

5.1. Interactions with $N_h \geq 28$

The charge carried away by protons and helium nuclei (ΔZ) can be calculated by the formula:

$$\Delta Z = C_{fr} C_\alpha \, (C_\pi N_h) \qquad [7]$$

where C_π accounts for the mixture of pions,

$C_\alpha = 1 + N_\alpha/(N_p+N_\alpha)$ and

C_{fr} accounts for the mixture of particles with $Z \geq 3$.

An estimation of the pion frequency (chapter 4) gives $C_\pi = 0.95 \pm 0.01$. The N_p/N_α ratio has been estimated using results from Refs.9,26 and 27 for particles with $E \leq 30$ MeV and from the experimental N_p/N_α ratio (=5) for $E > 30$ MeV. The result is $C_\alpha = 1.19 \pm 0.03$. From the value of $\langle N_h \rangle$ for interactions with $N_h \geq 28$ (33.3) and $\langle Z_{target} \rangle = 41.4$ we obtain $(C_{fr})_{min} \approx 0.94$. These estimations give $\Delta Z > 34$ and thus a very high degree of disintegration. Similar calculations for p-N interactions also show a high degree of breakup when $N_h \geq 28$ (28).

Table 2 shows the ratio $W = N(N_h \geq 28)/N(Ag\text{-}Br)$ for different kinds of incident nuclei. N(Ag-Br) is the number of collisions with Ag or Br targets. The percentage of Ag-Br collisions has been obtained,using the overlap cross section model for N-N interactions and experimental cross sections for interactions including hydrogen (8).

Table 2

Type of interaction		Number of stars	W(%)	Reference
Proton-nucleus	6.2 GeV	1769	2.1 ± 0.5	11
	9.6 GeV	1667	3.1 ± 0.6	28
	22.5 GeV	892	3.1 ± 0.8	11
	69 GeV	1040	3.0 ± 0.8	28
	200 GeV	1389	2.2 ± 0.5	29
Nucleus-nucleus	$3 \leq Z \leq 5$	295	9.3 ± 2.9	3,4,30,31 32,33,34 + this work
	$6 \leq Z \leq 9$	991	7.8 ± 1.5	
	$10 \leq Z \leq 15$	292	11.7 ± 3.7	
	$16 \leq Z \leq 26$	172	13.0 ± 5.3	

In p-N interactions there seems to be no energy dependence between 6 and 200 GeV. For light incident nuclei the number of total break up interactions increases with a factor 2-3 and for heavy incident nuclei ($Z \geq 10$) the factor is 4-5.

The target disintegration does not seem to affect the forward--backward asymmetry, $A_s = (N_{forw}-N_{backw})/(N_{forw}+N_{backw})$, of grey track-producing protons. A_s is 0.62 ± 0.07 for $N_h \geq 28$ and 0.61 ± 0.08 for the rest of the Ag-Br interactions. For N_h between 2 and 7, where the target nuclei are C, N or O almost exclusively (8), $A_s = 0.62 \pm 0.18$. This is not in agreement with the large difference found in the forward-backward ratio of grey prongs between interactions with $N_h \geq 28$ and $8 \leq N_h \leq 27$ in Ref. 4.

5.2. Multiplicities of Secondary Particles in Interactions with Different Degree of Disintegration

Table 3 shows characteristic features of interactions divided into five groups according to target- and projectile disintegration. Target nucleons knocked out in primary or secondary n-n and π-n collisions mainly receive an energy between 30 and 400 MeV. Table 3 indicates that about 20 % of the target nucleons in Ag-Br interactions are knocked out when the target nucleus or the projectile nucleus is moderately disintegrated ($N_h \leq 27$, $\Sigma Z_{fr}/Z_{inc} > 0.1$). A total target break up or a total projectile break up increases this number to about 40 %, and when both nuclei are totally disintegrated to about 50 %. The number of protons with $9 \leq E_p \leq 30$ MeV seems to be almost independent of the degree of disintegration of the interacting nuclei.

In Table 3 we can observe that the pion multiplicity increases with about the same factor (≈ 2) as the number of recoil

Table 3

Target		$\langle Z_{inc} \rangle$	$\langle Z_{fr} \rangle$	$\langle N_p$(9-30 MeV)$\rangle$	$\langle N_p$(30-400 MeV)$\rangle$	$\langle N_{\pi^\pm} \rangle$	$\langle \Theta_s^{\circ} \rangle$
Ag-Br	$N_h \geq 28$	17.7±1.3	1.6±0.5	4.1±0.5	17.7±1.5	30.3±7.1	28.9±1.0
Ag-Br	$N_h \leq 27$	19.7±1.0	8.4±0.5	3.0±0.3	7.8±1.5	16.4±4.0	22.2±0.9
C-N-O		19.8±1.0	11.3±1.4	0.5±0.2	1.7±0.3	6.2±2.2	15.5±1.1
Ag-Br	$\frac{\Sigma Z_{fr}}{Z_{inc}} \leq 0.1$	17.6±1.5	0.1±0.1	3.4±0.5	16.6±1.6	37.0±8.3	28.5±0.9
Ag-Br	$\frac{\Sigma Z_{fr}}{Z_{inc}} > 0.1$	19.6±1.0	8.9±1.1	3.3±0.3	8.6±1.0	13.7±3.3	22.1±3.8

protons when total breakups are compared with the rest of the Ag-Br interactions. In C-N-O collisions the number of pions per recoil proton is larger than in Ag-Br collisions. In order to explain these fenomena we turn to a comparison with p-N interactions.

5.3. Multiplicities of Secondary Particles in p-N and N-N interactions

In Table 4 we compare the ratio between N_b, N_g and $N_{\pi^\pm}$ in p-N and N-N interactions for different N_h-groups. Also the $N_{\pi^\pm}/N_g$ ratios are shown. The data from p-N interactions at 6.2 GeV have been taken from Ref. 11.

Table 4

	$N_h \leq 1$	$2 \leq N_h \leq 6$	$7 \leq N_h \leq 27$	$N_h \geq 28$
$N_b(N\text{-}N)/N_b(p\text{-}N)$	(1.4±0.7)	1.0±0.1	1.1±0.1	0.8±0.1
$N_g(N\text{-}N)/N_g(p\text{-}N)$	(1.1±0.5)	1.1±0.2	1.5±0.1	1.6±0.2
$N_{\pi^\pm}(N\text{-}N)/N_{\pi^\pm}(p\text{-}N)$	1.6±0.3	3.3±0.6	6.5±0.7	10.9±2.3
$N_{\pi^\pm}(p\text{-}N)/N_g(p\text{-}N)$		1.4±0.2	0.5±0.04	0.25±0.06
$N_{\pi^\pm}(N\text{-}N)/N_g(N\text{-}N)$		4.0±1.0	2.1±0.2	1.6±0.2

The pion multiplicity is only slightly larger in N-N interactions than in p-p and p-N interactions for $N_h \leq 1$. Bubble chamber results for p-p scattering at 6.2 GeV give $\langle N_{\pi^\pm} \rangle = 1.5$ (25), p-N results from Ref. 11 give $\langle N_{\pi^\pm} \rangle = 1.6 \pm 0.2$ and our result for N-N interactions is $\langle N_{\pi^\pm} \rangle = 2.6 \pm 0.4$. The mean energy per nucleon of the incident nuclei in the N-N sample is however slightly lower than 6.2 GeV. In order to get $N_{\pi^\pm}$ in p-N interactions we have assumed that the number of surviving incident protons is 0.65 ± 0.1 per collision. The $N_{\pi^\pm}$ value in N-N inter-

actions has been obtained using the expression:

$$N_{\pi\pm} = N_s - (Z_{inc} - \Sigma Z_{fr}) \qquad [8]$$

where Z_{fr} is the charge of relativistic fragments with $Z \geq 2$. This means that the total charge exchange between protons and neutrons has been neglected.

For increasing N_h interesting results are obtained. In spite of an almost constant $\langle N_b \rangle$-ratio and a very slow increase in the $\langle N_g \rangle$-ratio the pion multiplicity ratio increases very fast. For total breakups in Ag and Br the pion multiplicity is about ten times larger in N-N than in p-N interactions. The number of produced pions per emitted recoil proton decreases more rapidly in p-N than in N-N interactions.

The perturbation from the number of fast target protons ($E > 400$ MeV) and the number of slow recoil protons ($E < 40$ MeV) can not make the ratios in Table 4 fall outside the limits of error.

5.4. Production of Secondary Particles in p-N and N-N Interactions

Comparisons between p-N and N-N interactions reflect the larger number of first nucleon-nucleon encounters in N-N collisions. It is reasonable to assume that the different behaviour of p-N and N-N interactions is more pronounced in collisions with a large disintegration of the target nuclei. We have found that the average production of pions increases much faster in N-N than in p-N interactions with increasing N_h. The mean pion multiplicity per recoil proton in N-N collisions seems to be affected very little by the degree of disintegration of the interacting nuclei. In p-N collisions there is however a more rapid decrease in $N_{\pi^\pm}/N_g$ for increasing N_h.

In the N-N sample the interactions with a large target disintegration is no homogenous group but consists of events with large variation in the pion multiplicity. This is is agreement with the cosmic ray energy spectrum and the fact that the number of events with $N_h \geq 28$ is energy independent. Events with a large impact parameter and small pion multiplicity can also develop a large cascade and thus a high degree of target disintegration.

We have some events in our N-N sample with a very large pion multiplicity. The energy necessary to explain the large multiplicity is much too high to agree with the logtg Θ distribution of pions and the cosmic ray energy spectrum. In these extreme events a large transverse momentum is transferred to the majority of the projectile protons.

We are grateful to the U.S. Office of Naval Research for the exposure of the emulsion stacks. Thanks are also due to Miss B. Lindkvist for the processing of the emulsions. The financial support from the Swedish Atomic Research Council is gratefully acknowledged.

References

1. Harp, G.D., Miller, J.M., Berne, B.J.: Phys. Rev. 165, 1166 (1968).

2. Harp, G.D., Miller, J.M.: Phys. Rev. C3, 1847 (1971).

3. Andersson, B., Otterlund, I., Kristiansson, K.: Arkiv Fysik 31, 527 (1966).

4. Gagarin, Yu. F., Ivanova, N.S., Kulikov, V.N.: Sov. J. Nucl. Phys. 11, 698 (1970).

5. Epherre, M., Gradsztajn, E., Klapisch, R., Reeves, H.: Nucl. Phys. A 139, 545 (1969).

6. Glassgold, A.E., Heckrotte, W., Watson, M.: Annals of Phys. 6, 1 (1959).

7. Feshbach, H., Huang, K.: Phys. Lett. 47 B, 300 (1973).

8. Jakobsson, B., Kullberg, R., Otterlund, I.: Z. Physik 268, 1 (1974).

9. Hyde, E.K., Butler, G.W., Poskanzer, A.M.: Phys. Rev. C4, 1759 (1971).

10. Sutter, R.J., Friedes, J.L., Palevsky, H., Bennett, G.W., Igo, G.J., Simpson, W.D., Phillips, G.C., Corley, D.M., Wall, N.S., Stearns, R.L.: Phys. Rev. Lett. 19, 1189 (1967).

11. Winzeler, H.: Nucl. Phys. 69, 661 (1965).

12. Goryachikh, A.A., Takibaev, Zh. S., Titova, N.S., Shalagina, E.V.: Sov. J. Nucl. Phys. 13, 729 (1971).

13. Lock, W.O., March, P.V., McKeague, R.: Proc. Roy. Soc. A 231, 368 (1955).

14. Barashenkov, V.S., Beliakov, V.A., Glagolev, V.V., Dalkhazhov, N., Yao Tsyng Se, Kirilova, L.F., Lebedev, R.M., Maltsev, V.M., Markov, P.K., Shafranova, M.G., Tolstov, K.D., Tsyganov, E.N., Wang Shou Feng: Nucl. Phys. 14, 522 (1959/60).

15. Metropolis, N., Bivins, R., Storm, M., Miller, J.M., Friedlander, G., Turkevich, A.: Phys. Rev. 110, 204 (1958).

16. King, D.T.: Phys. Rev. 188, 1731 (1969).

17. Bertini, H.W.: Phys. Rev. 188, 1711 (1969).

18. Almeida, S.P., Rushbrooke, J.G., Scharenguivel, J.H., Behrens, M., Blobel, V., Borecka, I., Dehne, H.C., Diáz, J., Knies, G., Schmitt, A., Strömer, K., Swanson, W.P.: Phys. Rev. 174, 1638 (1968).

19. Yekutieli, G., Toaff, S., Shapira, A., Ronat, E.E., Luons, L., Eisenberg, Y., Carnel, Z., Fridman, A., Maurer, G., Strub, R., Voltolini, C., Cüer, P., Grunhaus, J.: Nucl. Phys. B 18, 301 (1970).

20. Fickinger, W.J., Pickup, E., Robinson, D.K., Salant, E.O., Phys. Rev. 125, 2082 (1962).

21. Eisner, A.M., Hart, E.L., Louttit, R.I., Morris, T.W.: Phys. Rev. 138, B 670 (1965).

22. Krisch, A.D.: Phys. Rev. Lett. 19, 1149 (1967).

23. Wong, C.Y., Welton, T.A.: To be published.

24. Gibbs, R.E., Florian, J.R., Kirkpatrick, L.D., Lord, J.J., Martin, J.W.: To be published.

25. Morrison, D.R.O.: Proc. 4:th Int. Conf. on High Energy Collisions, Oxford 1972.

26. Kullberg, R., Otterlund, I., Resman, R.: Physica Scripta 5, 5 (1972).

27. Dostrovsky, I., Rabinowitz, P., Bivins, R.: Phys. Rev. 111, 1659 (1958).

28. Tolstov, K.D., Khoshmukhamedov, R.A.: JINR P1-6897 (1973).

29. Barcelona-Batavia-Belgrade-Bucharest-Lund-Lyons-Montreal--Nancy-Ottawa-Rome-Strasbourg-Valencia Collaboration. Private communication.

30. Rajopadhye, V.Y., Waddington, C.J.: Phil. Mag. 3, 19 (1958).

31. Maeda, Y.: J. Phys. Soc. (Japan) 18, 945 (1963).

32. Fowler, P.H., Hillier, R.R., Waddington, C.J.: Phil. Mag. 2, 293 (1957).

33. Cester, R., Debenedetti, A., Garelli, C.M., Quassiati, B., Tallone, L., Vigone, M.: Nuovo Cimento 7, 371 (1958).

34. Tzuzuki, Y.: J. Phys. Soc. (Japan) 16, 2131 (1961).

Figure Captions

1. Angular distributions of protons in the energy intervals a) 9-30 MeV b) 30-235 MeV c) 235-400 MeV.

2. Angular distributions of protons ($30 \leq E < 400$ MeV) in N-N interactions and of grey tracks in p-N interactions. The curves are fits of exponential distributions to the experimental samples (in the N-N interactions only for $\cos \Theta < 0.8$).

3. Energy distributions of protons in N-N interactions ($9 \leq E < 400$ MeV) and in p-N interactions ($25 \leq E < 400$ MeV) normalized to the same number of particles in the interval 50-400 MeV.

4. Energy distributions of knock on protons from N-N and p-N interactions (Ag-Br targets) in the angular intervals a) $\Theta < 30^{\circ}$ and b) $70^{\circ} \leq \Theta < 110^{\circ}$.

5. Logtg Θ distributions of pions produced in p-p interactions at 10 GeV, assuming different analytic expressions of the cm momentum distribution.

6. Logtg Θ distributions of pions and fast protons emitted in p-p interactions at 2 and 10 GeV and of protons emitted from excited residual projectile nuclei in N-N interactions.

7. Experimental logtg Θ distributions of shower particles in N-N interactions. Curves in a-e are pion distributions from p-p interactions normalized to the experimental number of pions in the N-N interactions. The curve in f is

an evaporation distribution normalized to the experimental number of particles with logtg $\theta < -1.4$.

8. Experimental logtg θ distributions of shower particles in the three largest stars. The curves are pion distributions from 10 GeV p-p interactions.

9. Angular distributions of shower particles in N-N and p-N interactions. The curve is a pion distribution from p-p interactions assuming isotropic cm emission.

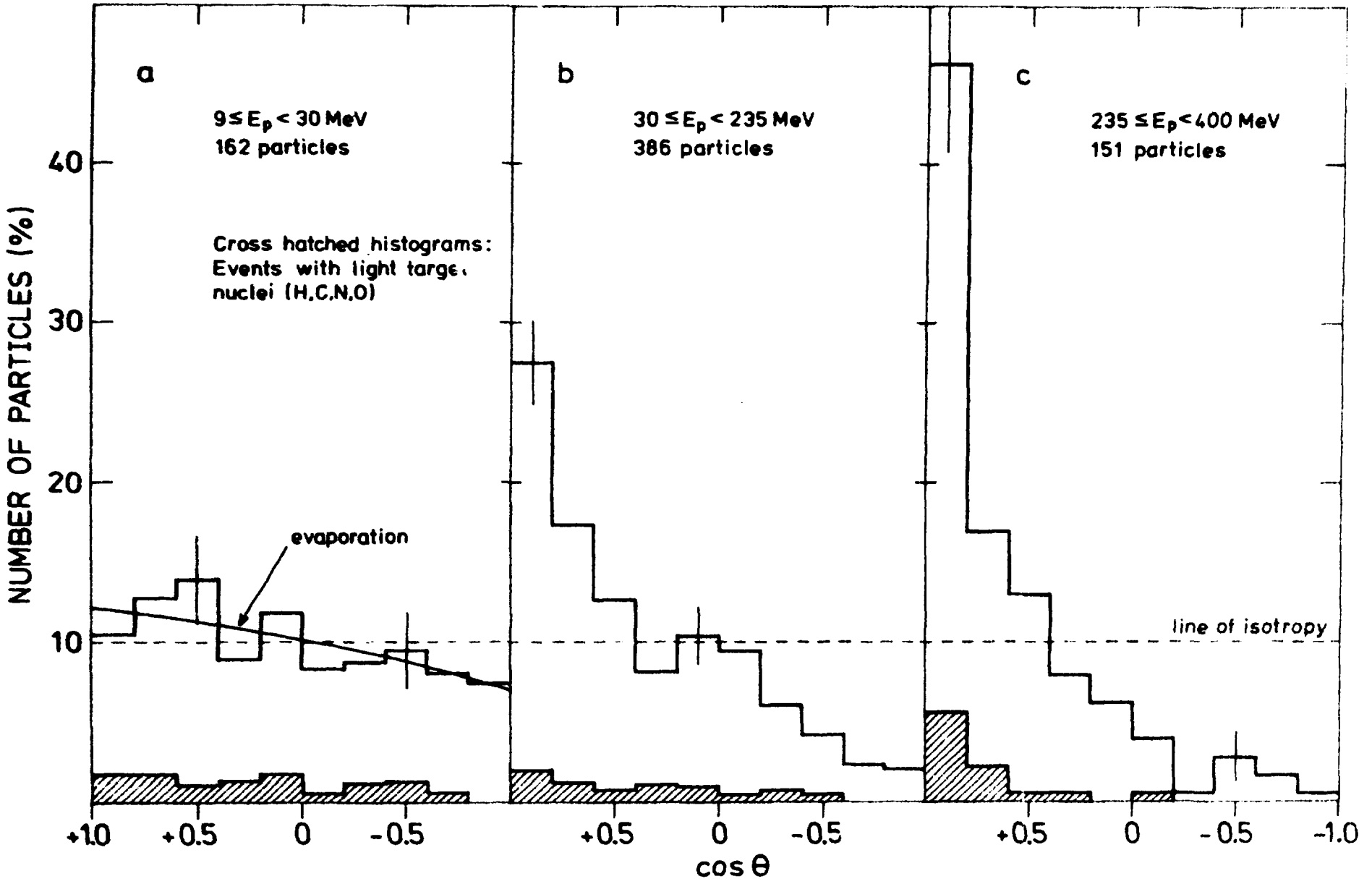
a
b
c
9 ≤ Ep < 30 MeV
162 particles
30 ≤ Ep < 235 MeV
386 particles
235 ≤ Ep < 400 MeV
151 particles
Cross hatched histograms:
Events with light target
nuclei (H,C,N,O)
evaporation
line of isotropy
NUMBER OF PARTICLES (%)
40
30
20
10
+1.0
+0.5
0
-0.5
+0.5
0
-0.5
+0.5
0
-0.5
-1.0
cos θ

Fig. 1

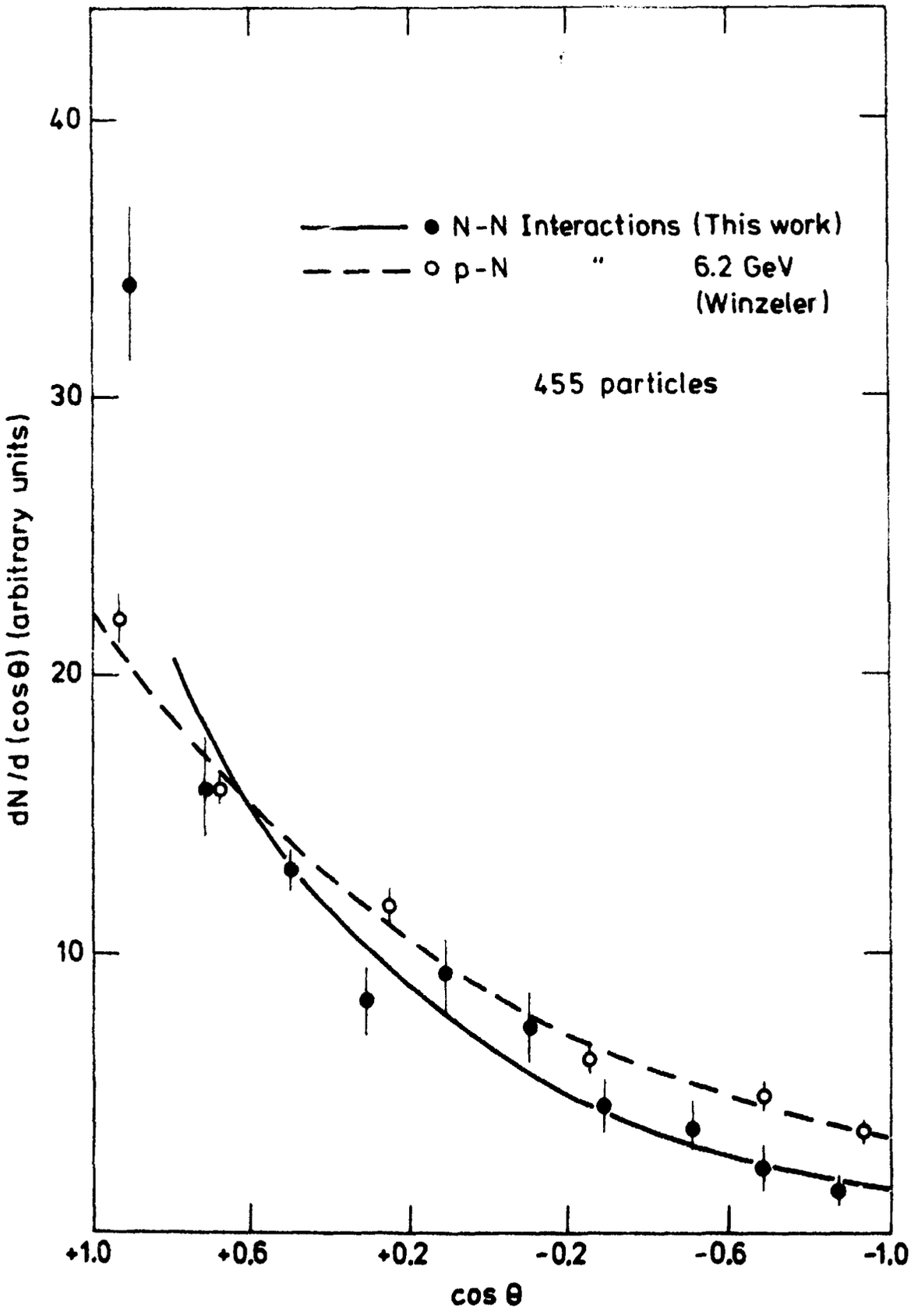
40
30
20
10
dN/d (cosθ) (arbitrary units)
● N-N Interactions (This work)
o p-N " 6.2 GeV
(Winzeler)
455 particles
+1.0
+0.6
+0.2
-0.2
-0.6
-1.0
cos θ

Fig.2

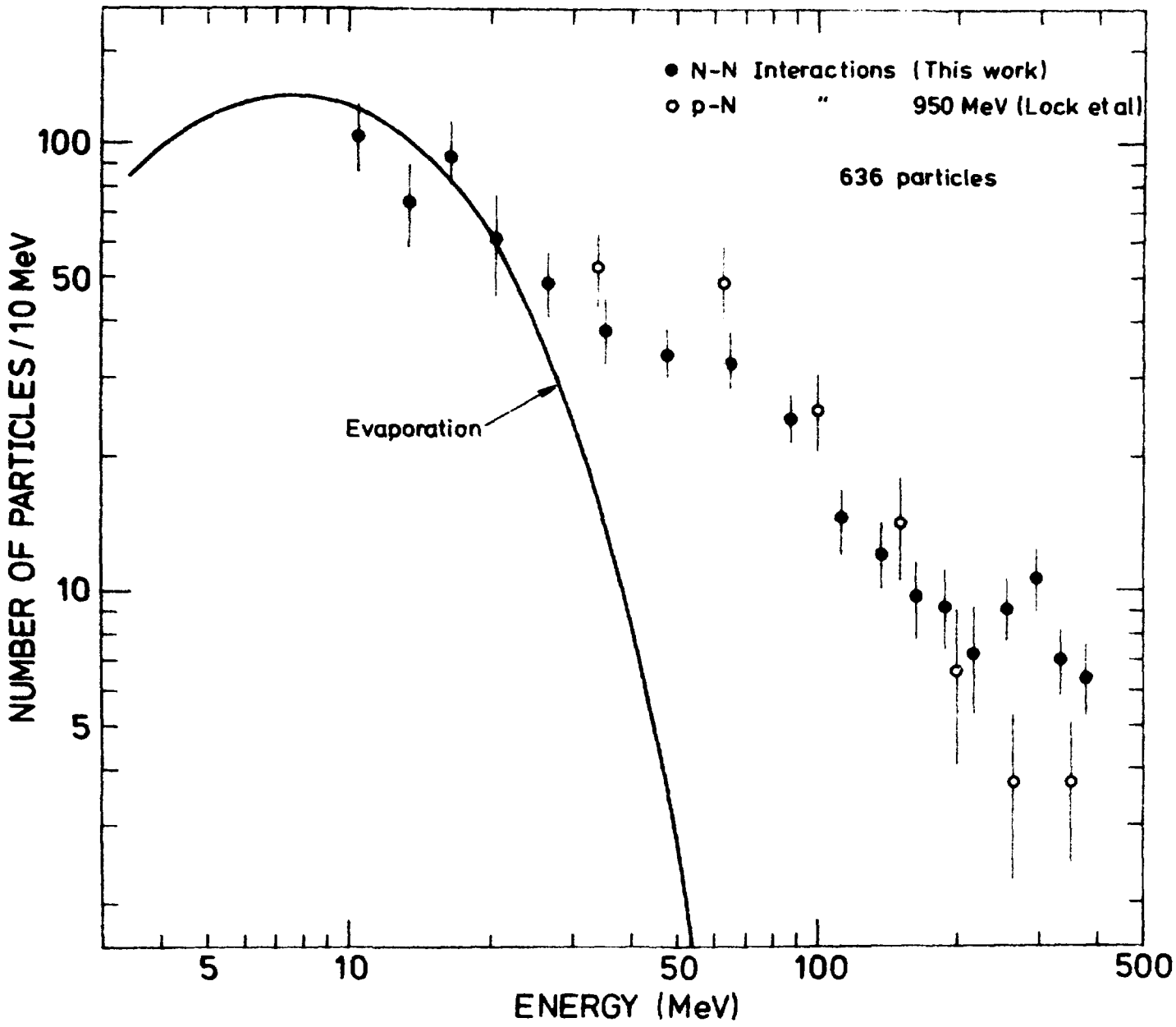
● N-N Interactions (This work)
○ p-N " 950 MeV (Lock et al)
636 particles
Evaporation
NUMBER OF PARTICLES / 10 MeV
100
50
10
5
5
10
50
100
500
ENERGY (MeV)

Fig.3

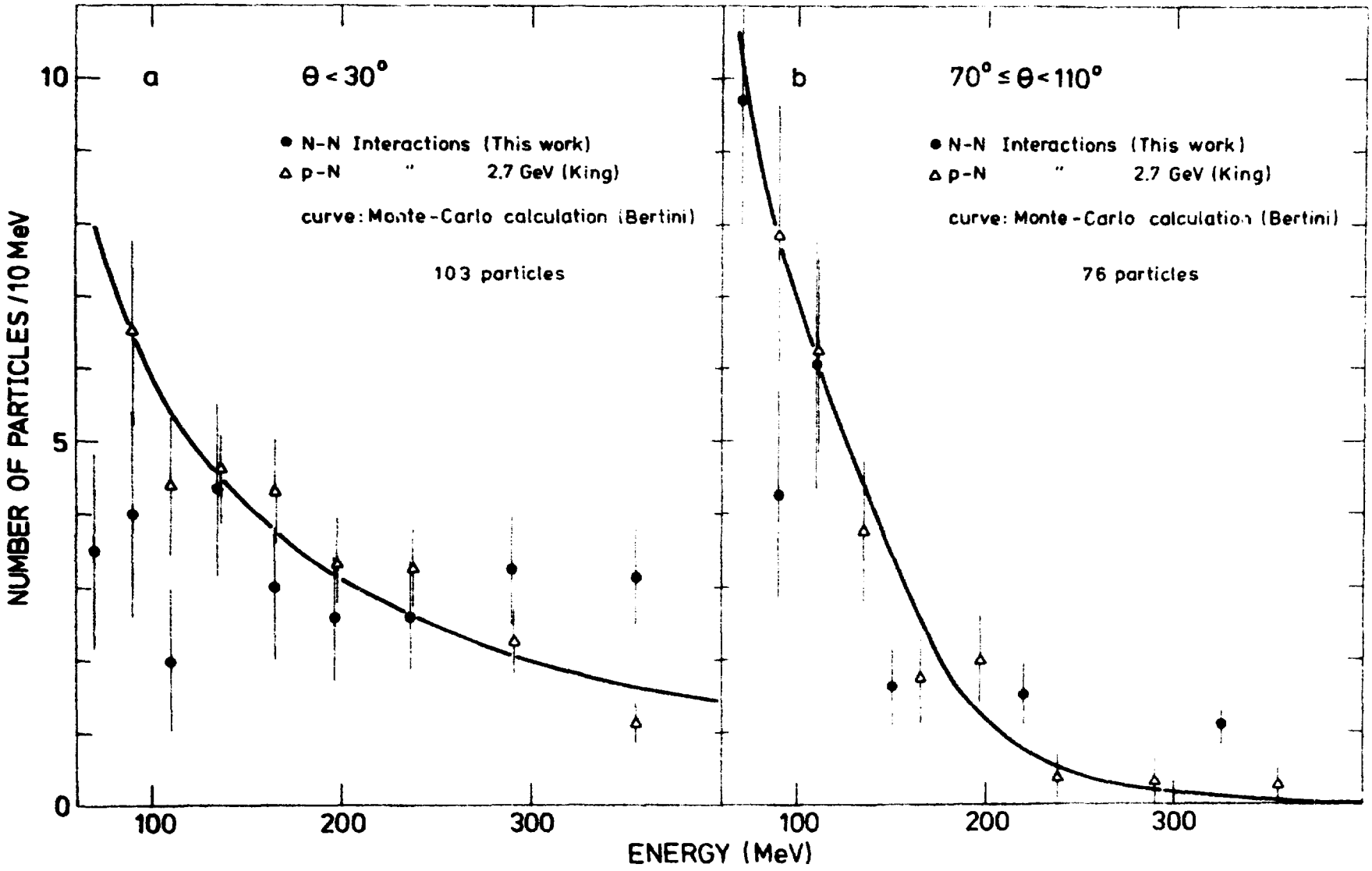
a
θ < 30°
● N-N Interactions (This work)
△ p-N " 2.7 GeV (King)
curve: Monte-Carlo calculation (Bertini)
103 particles
b
70° ≤ θ < 110°
● N-N Interactions (This work)
△ p-N " 2.7 GeV (King)
curve: Monte-Carlo calculation (Bertini)
76 particles
NUMBER OF PARTICLES / 10 MeV
ENERGY (MeV)
0
5
10
100
200
300

Fig. 4

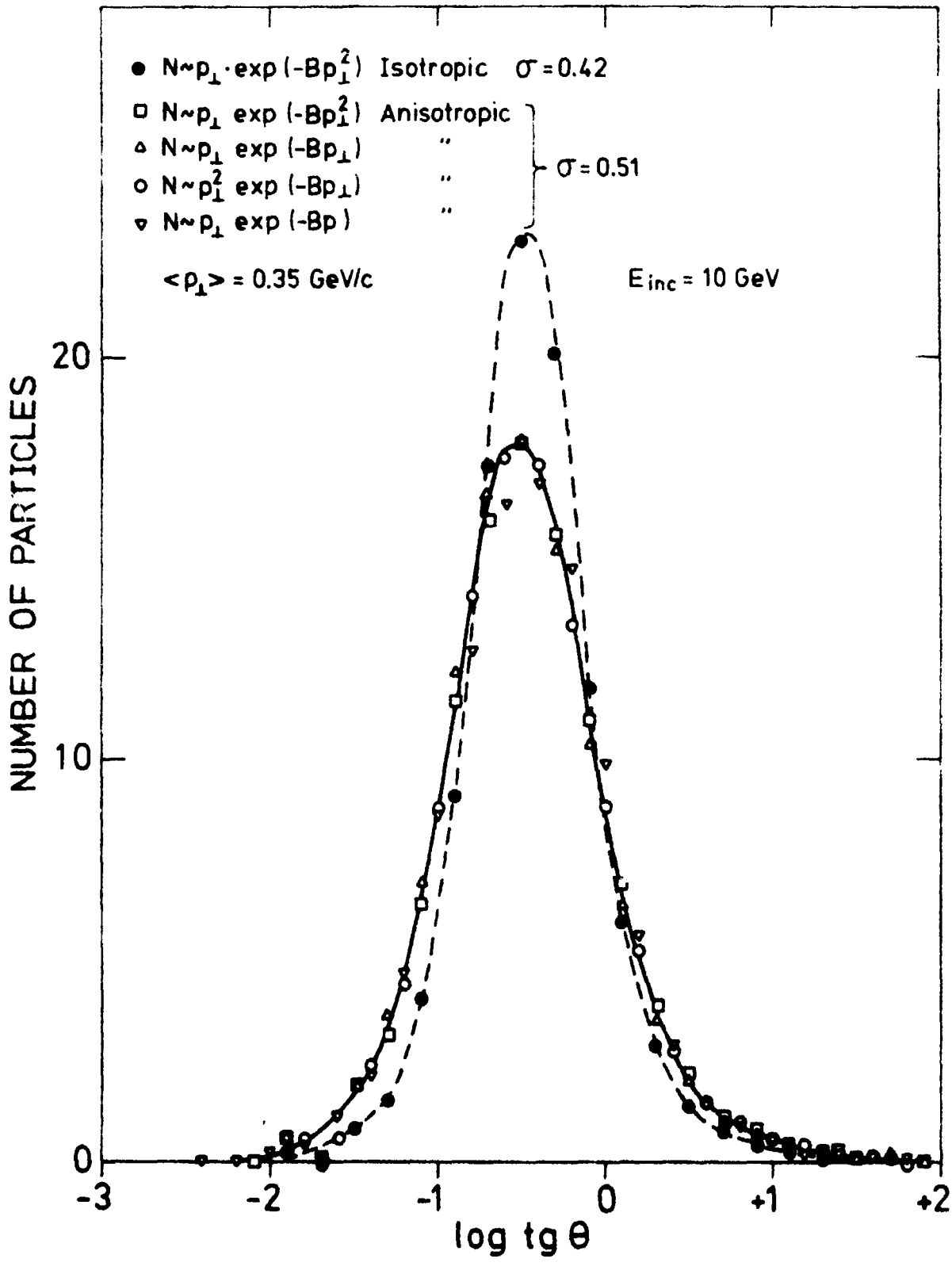
● N~p⊥·exp(-Bp⊥²) Isotropic σ=0.42
□ N~p⊥ exp(-Bp⊥²) Anisotropic
△ N~p⊥ exp(-Bp⊥) "
○ N~p⊥² exp(-Bp⊥) "
▽ N~p⊥ exp(-Bp) "
σ=0.51
<p⊥> = 0.35 GeV/c
E inc = 10 GeV
NUMBER OF PARTICLES
20
10
0
-3
-2
-1
0
+1
+2
log tg θ

Fig.5

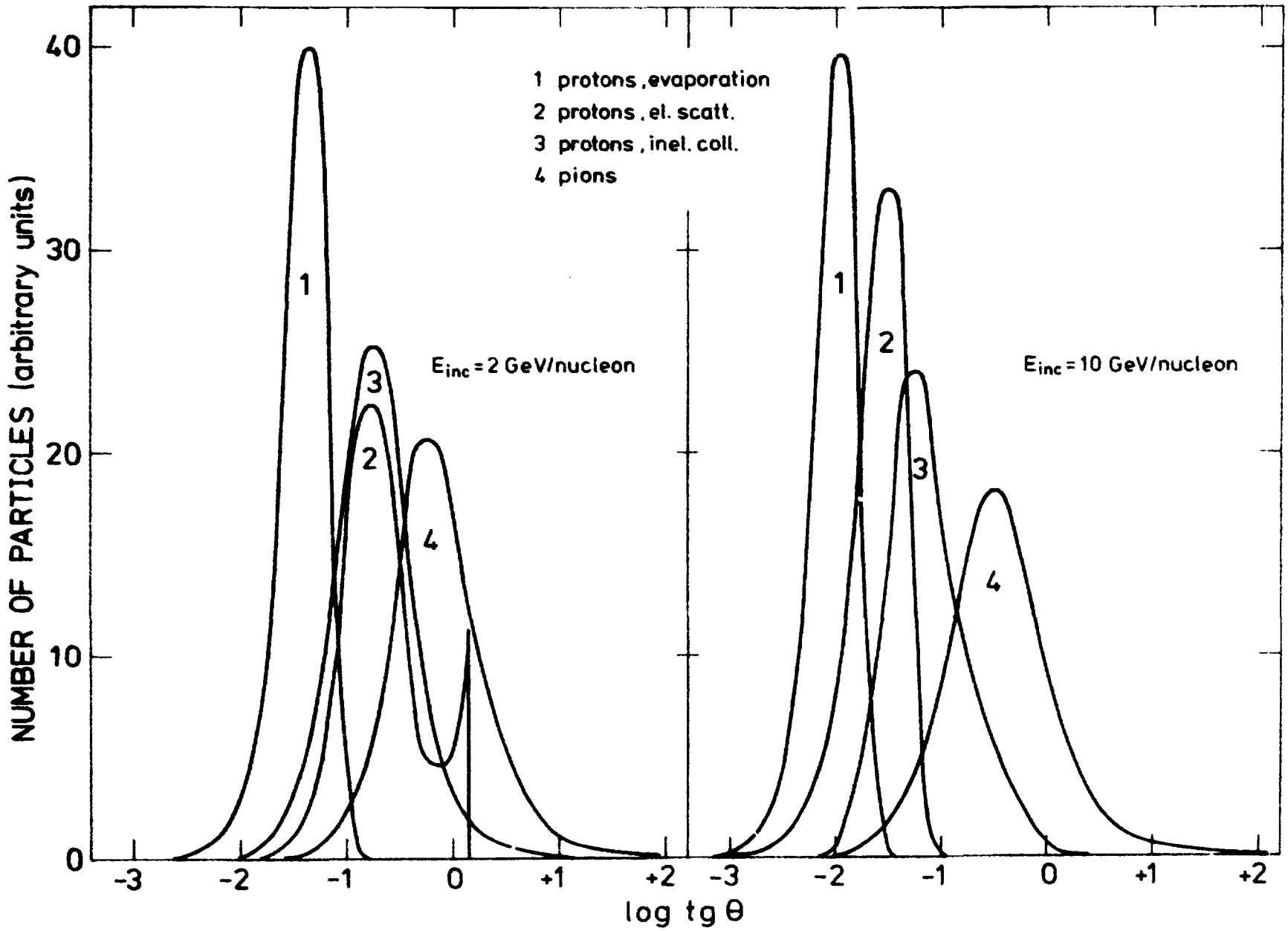
1 protons, evaporation
2 protons, el. scatt.
3 protons, inel. coll.
4 pions
E_{inc} = 2 GeV/nucleon
E_{inc} = 10 GeV/nucleon
NUMBER OF PARTICLES (arbitrary units)
log tg θ
0
10
20
30
40
-3
-2
-1
0
+1
+2

Fig.6

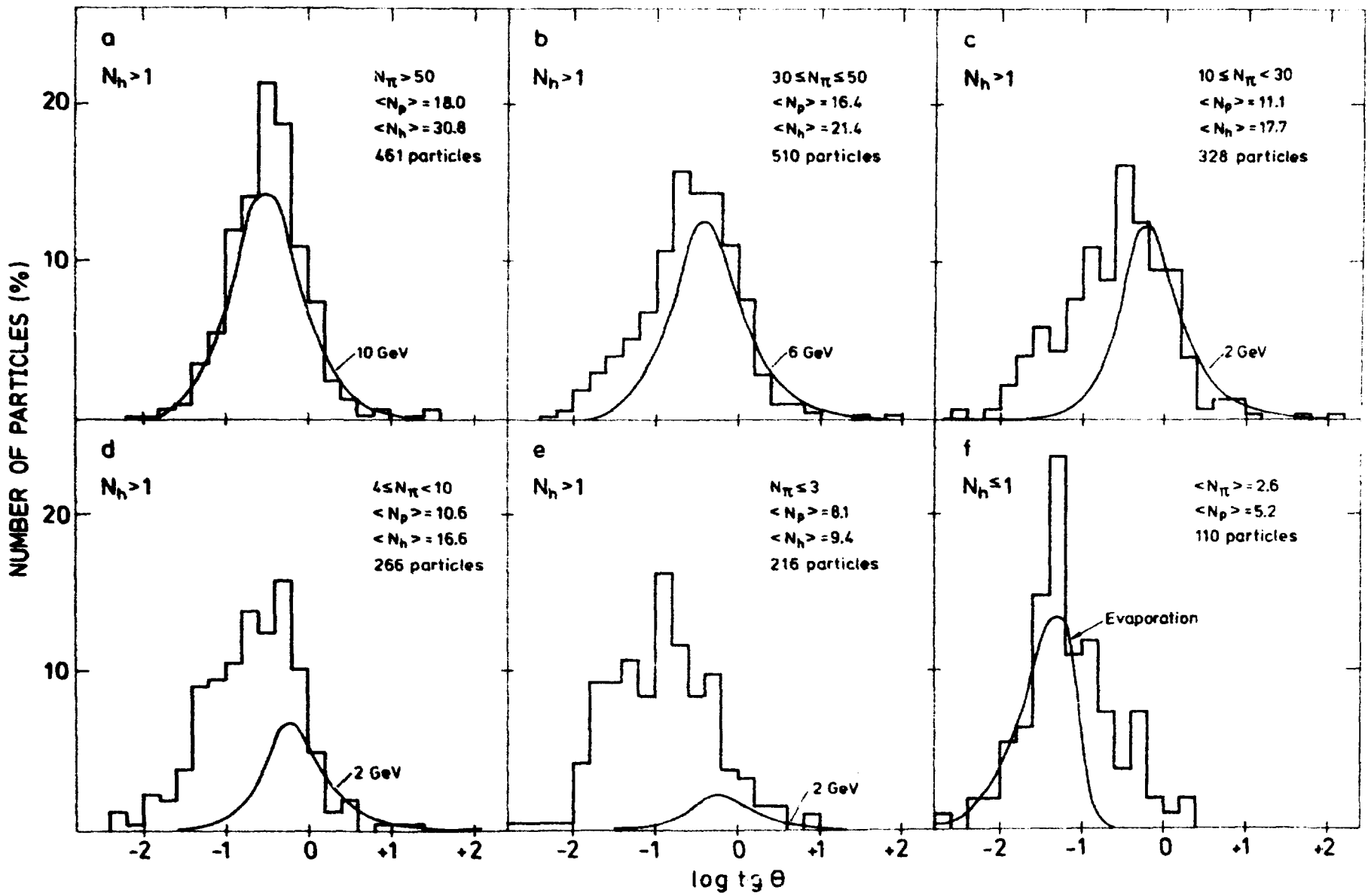
a
$N_h > 1$
$N_\pi > 50$
$\langle N_p \rangle = 18.0$
$\langle N_h \rangle = 30.8$
461 particles
10 GeV
b
$N_h > 1$
$30 \leq N_\pi \leq 50$
$\langle N_p \rangle = 16.4$
$\langle N_h \rangle = 21.4$
510 particles
6 GeV
c
$N_h > 1$
$10 \leq N_\pi < 30$
$\langle N_p \rangle = 11.1$
$\langle N_h \rangle = 17.7$
328 particles
2 GeV
d
$N_h > 1$
$4 \leq N_\pi < 10$
$\langle N_p \rangle = 10.6$
$\langle N_h \rangle = 16.6$
266 particles
2 GeV
e
$N_h > 1$
$N_\pi \leq 3$
$\langle N_p \rangle = 8.1$
$\langle N_h \rangle = 9.4$
216 particles
2 GeV
f
$N_h \leq 1$
$\langle N_\pi \rangle = 2.6$
$\langle N_p \rangle = 5.2$
110 particles
Evaporation
NUMBER OF PARTICLES (%)
20
10
-2
-1
0
+1
+2
log tg θ

Fig.7

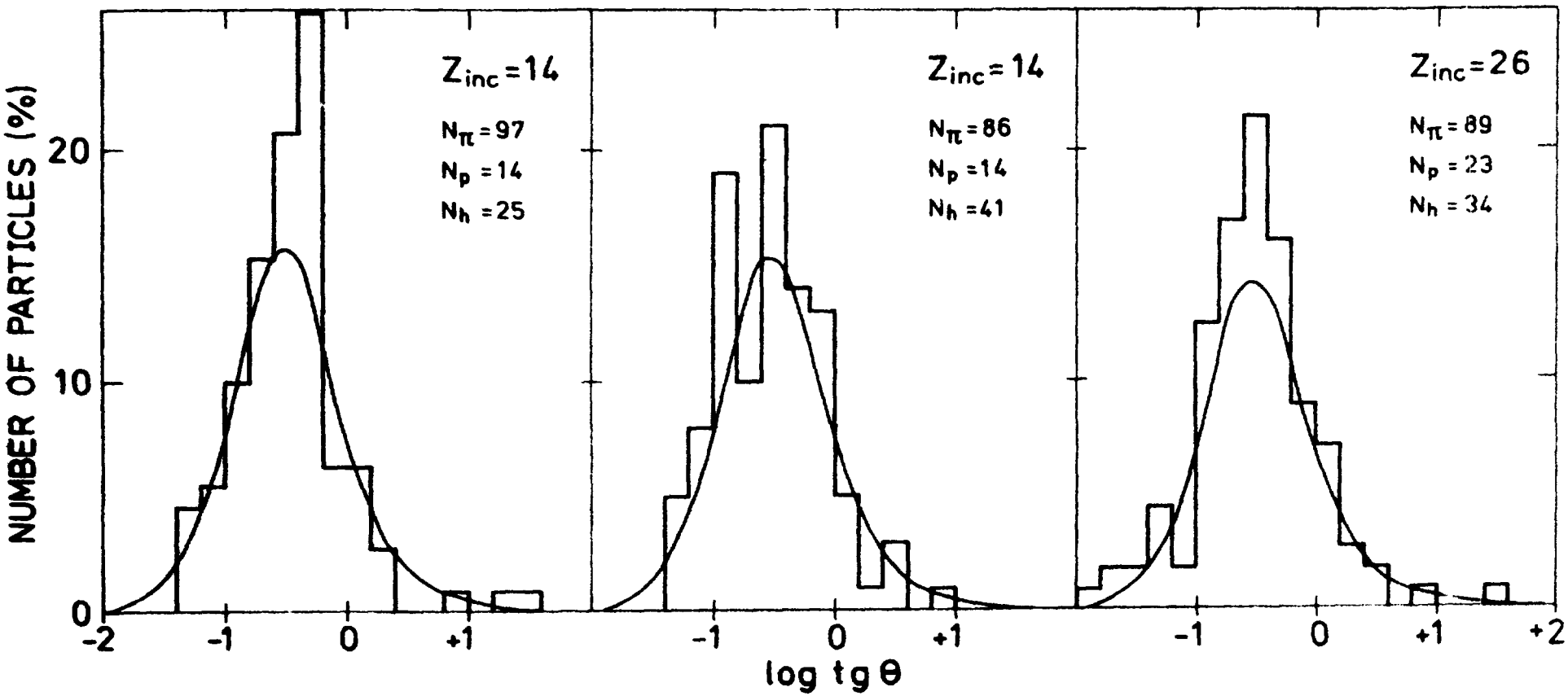
$Z_{inc}=14$
$N_\pi=97$
$N_p=14$
$N_h=25$
$Z_{inc}=14$
$N_\pi=86$
$N_p=14$
$N_h=41$
$Z_{inc}=26$
$N_\pi=89$
$N_p=23$
$N_h=34$
NUMBER OF PARTICLES (%)
0
10
20
-2
-1
0
+1
+2
log tg θ

Fig.8

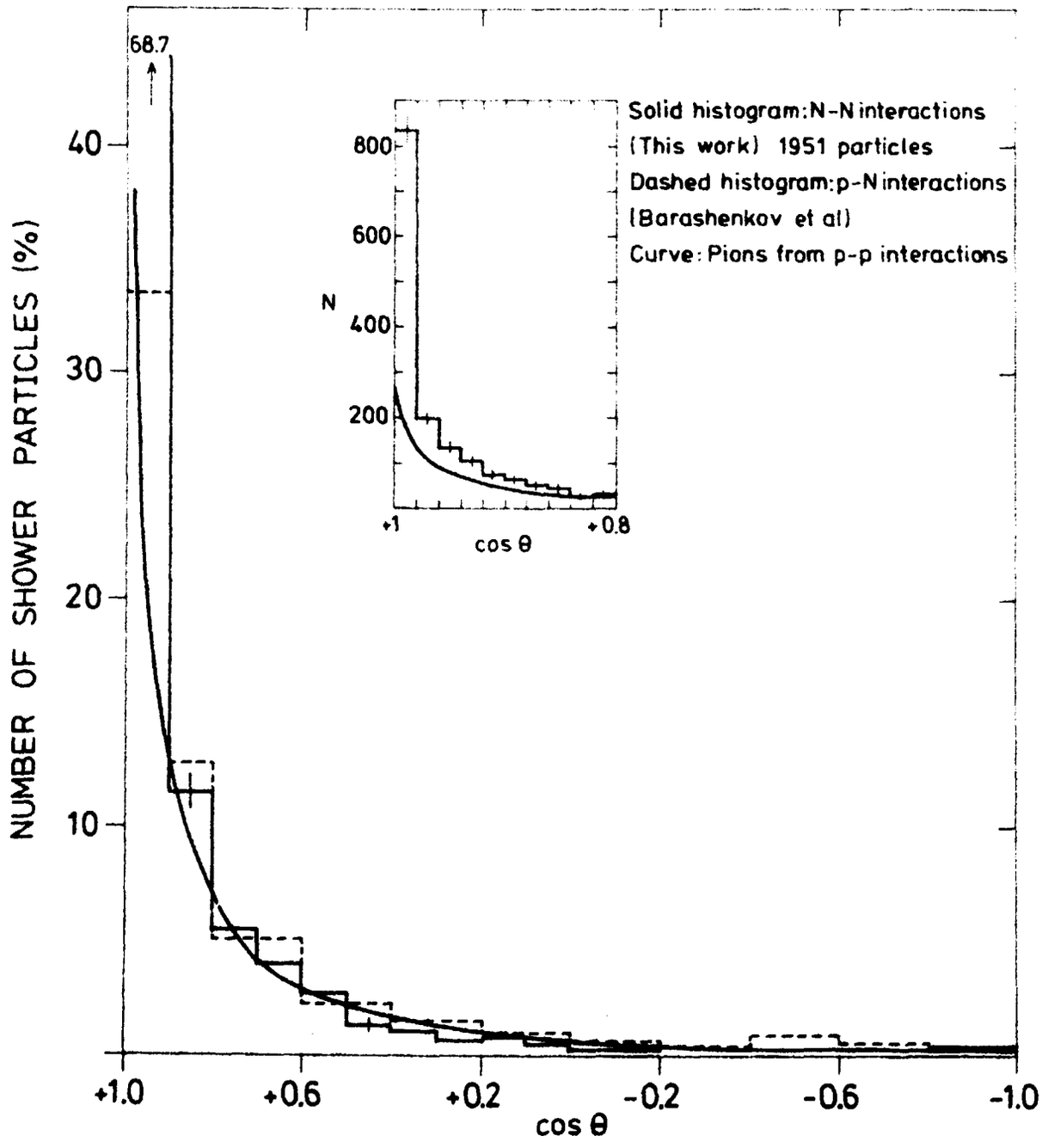
68.7
40
30
20
10
NUMBER OF SHOWER PARTICLES (%)
+1.0
+0.6
+0.2
-0.2
-0.6
-1.0
cos θ
800
600
400
200
N
+1
+0.8
cos θ
Solid histogram: N-N interactions
(This work) 1951 particles
Dashed histogram: p-N interactions
(Barashenkov et al)
Curve: Pions from p-p interactions

Fig.9